

An extensible methodology for creating realistic anthropomorphic digital phantoms for quantitative imaging algorithm comparisons and validation

Ryan J Bosca¹ and Edward F Jackson¹

¹Medical Physics, University of Wisconsin - Madison, Madison, WI, United States

PURPOSE: Assessing and mitigating the numerous sources of bias and variance associated with the acquisition and analysis of quantitative imaging biomarker data is paramount to their applications in clinical research and clinical practice. While substantial efforts have been made to evaluate and mitigate sources of bias and variance associated quantitative acquisition strategies, relatively little work has been performed to develop a means of comparing and validating, in a realistic setting with known “ground truth”, the analysis algorithms used to derive quantitative imaging biomarker results. Digital reference objects (DROs) to date have consisted primarily of grid-based DICOM images (with grids on the order of 10x10 voxels) that contain data corresponding to a range of quantitative model parameters, for example digital perfusion phantoms^{1,2} and the relaxometry and pharmacokinetic (PK) phantoms developed by Barboriak *et al.*³. As the sophistication and accuracy of digital anthropomorphic phantoms improves⁴, the ability to validate quantitative imaging algorithms, especially in the context of highly heterogeneous pathology, becomes possible. To that end, we have developed a methodology for creating realistic DROs to evaluate the biases and variances associated with the algorithms used in quantitative imaging, specifically pharmacokinetic (PK) modeling of dynamic contrast agent enhanced MRI (DCE-MRI) data. The proposed framework, however, can be generalized to other MR-based quantitative imaging biomarkers.

METHODS: A discretized digital anthropomorphic phantom of the brain^{4,6} was used as a template to synthesize a 4D DCE-MRI acquisition of a patient with a glioblastoma (GB). All indexed normal tissues (*i.e.*, gray matter, white matter, blood vessels, *etc.*) of the digital object were assigned the model parameters summarized in Table 1. To create the synthetic tumor, DCE-MRI data from a GB patient was retrospectively analyzed, producing maps for K^{trans} , v_e , and v_p using the general kinetic model (GKM)⁷. An enhancement threshold of 50% was manually defined to segment the tumor and additional morphological operations were used to clean jagged edge pixels. The digital phantom was then registered to the DCE-MRI volume using rigid image registration. Following co-registration, the segmented tumor volume was used to replace the respective voxels in the digital phantom with the GKM parameters estimated from the patient data. Using a VIF⁸ and the assigned DRO model parameters, voxel-by-voxel contrast agent concentration time courses were calculated for 330 frames of a 330s digital study using the general kinetic mode. These concentrations were converted to signal intensity assuming a perfectly spoiled, steady-state gradient echo sequence using: TR=5ms, FA=30°, and the assumption that $TE \ll T_2^*$. All images were exported subsequently in DICOM format and analyzed using the open-source quantitative imaging analysis tool QUATTRO⁹. A Bland-Altman analysis was performed on the tumor voxels to evaluate the biases.

RESULTS: An example cross-section of the PK parameter maps used to synthesize the tumor enhancement is displayed in Figure 1. Figure 2 illustrates the simulated imaging volume in a post-contrast phase of the digital study. The synthetic enhancing tumor (and blood vessels), which exhibits substantial heterogeneity in contrast uptake surrounding the fluid-filled post-surgical cavity, can be easily seen in the first eight slices of the volume. The gray-white matter contrast, resulting from differences in blood volume, is also readily apparent. The limits of agreement were found to be -0.076 and 0.004 min⁻¹ for K^{trans} , -0.047 and 0.0052 for v_e , and -0.090 and -0.0035 for v_p , suggesting minimal bias for K^{trans} and v_e while those biases for v_p are on the order of the 100%. On average, the true value of v_p for the synthetic tumor was approximately 0.03. Small fluctuations in the estimate of this parameter likely resulted in the larger observed biases of v_p compared to K^{trans} and v_e .

CONCLUSIONS: We have demonstrated a methodology, using freely available digital phantom and VIF data, that allows straightforward creation of a DRO capable of capturing the spatial heterogeneity encountered ubiquitously *in vivo*. Such objects are particularly important when validating quantitative imaging algorithms that employ spatial processing, such as neighborhood-based filtering or spatial models. Current DROs, based on grid patterned DICOM data, do not allow such assessments in an anatomically and physiologically relevant manner. Moreover, the proposed methodology is easily extensible to any number of other MRI-based quantitative imaging acquisition and analysis techniques and/or pathological processes, and noise models can be easily incorporated.

| Tissue | K^{trans} (min ⁻¹) | v_e (%) | v_p (%) | T_{10} (ms) |
|--------------|----------------------------------|-----------|-----------|---------------|
| CSF | 0 | 0 | 0 | 2750 |
| Gray Matter | 0 | 20 | 2 | 1820 |
| White Matter | 0 | 20 | 4 | 1084 |
| Fat | 0 | 0 | 0 | 260 |
| VIF | 0 | 0 | 100 | 1440 |
| GB | 0.03-0.6 | 0.1-60 | 0.1-10 | 1000 |

Table 1. Modeling parameters used to generate tissue contrast concentration time courses.

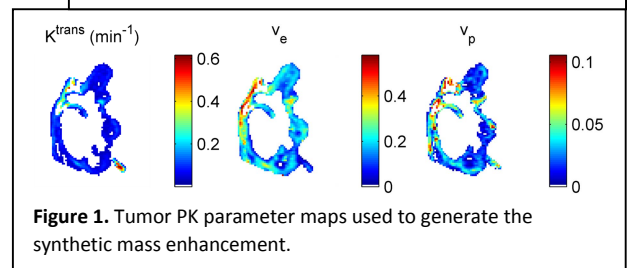


Figure 1. Tumor PK parameter maps used to generate the synthetic mass enhancement.

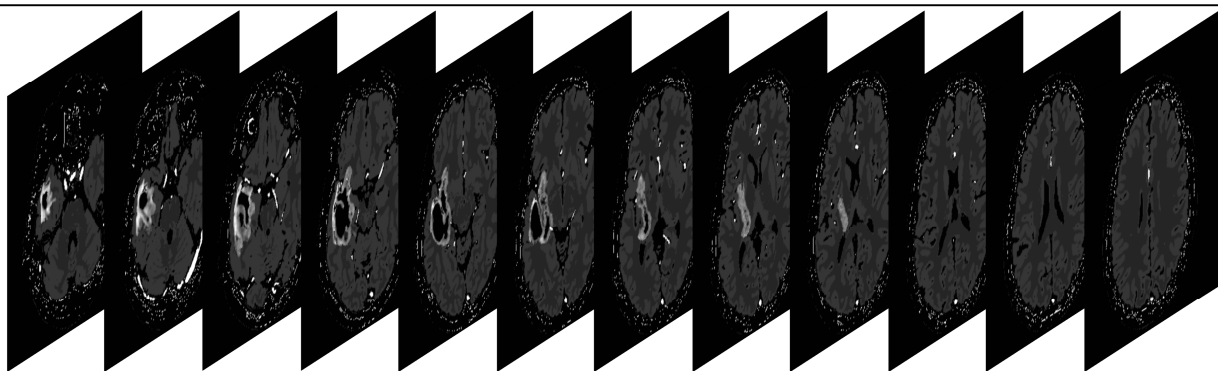


Figure 2. Post-enhancement volume showing the heterogeneous synthetic within normal tissue

References: [1] Østergaard L *et al.*, MRM 1996; 36(5): 715-725. [2] Kudo K *et al.* Radiology 2013; 267(1):201-2011.

[3] <https://dmlab.duhs.duke.edu/modules/QIBAcontent/index.php?id=1>. [4] Aubert-Broche B *et al.* NeuroImage 2006; 32(1): 138-145. [5] Kwan R *et al.*, Vis Biomed Comput 1996; 1131:135-140. [6] Kwan R *et al.*, IEEE Trans. Med. Imaging 1999; 18(11):1085-1097. [7] Tofts P *et al.*, JMRI 1999; 10: 223-232. [8] Barboriak *et al.* JMRI 2008; 27(6): 1388-1398. [9] Bosca RJ *et al.* Med Phys 2014; 41:380.